

# Growth of Carbon Clusters

## The Simplest Process, $2C_1 \rightarrow C_2$ , observed *via* Spectrometry and Chemical Reaction

Akihiro Wakisaka,\* J. J. Gaumet, Yukio Shimizu\* and Yukio Tamori

National Institute for Resources and Environment, Onogawa 16-3, Tsukuba, Ibaraki 305, Japan

Hideki Sato and Katsumi Tokumaru\*

Department of Chemistry, University of Tsukuba, Tsukuba, Ibaraki 305, Japan

A graphite sample has been irradiated with a YAG laser under an argon atmosphere. The emission due to the  $C_2(d^3\Pi_g \rightarrow a^3\Pi_u)$  Swan band was observed with a decay time 20 times the intrinsic lifetime of  $C_2(d^3\Pi_g)$ . In the presence of benzene, which reacts with  $C_1$ , the observed decay time of the  $C_2$  Swan band decreased with increasing benzene around the graphite. Furthermore, the reaction products between benzene and  $C_1$  or  $C_2$  were identified and their distribution varied remarkably with benzene concentration. From these results, the simplest growth process of carbon clusters,  $2C_1 \rightarrow C_2$ , was confirmed experimentally. Comparing the emission spectra from the irradiated graphite surface under an argon atmosphere and under vacuum, the collisional relaxation of  $C_1$  with argon was found to be indispensable to the growth process.

Since the discovery of the production of various carbon clusters, especially fullerenes, by laser vaporization<sup>1</sup> or electric discharge of graphite electrodes,<sup>2</sup> considerable attention has been paid to the structure and reactivity of carbon clusters. The effect of the carbon-cluster size on its photofragmentation<sup>3,4</sup> and chemical reactivity with gaseous molecules<sup>5–8</sup> has been investigated.

Much interest has been paid to the mechanism of the formation of carbon clusters. It will be essential for the control of carbon cluster formation. However, it is surprising to find very little direct experimental evidence on the growth of a carbon cluster.<sup>9</sup>

We reported recently that  $C_2$  formation from  $C_1$ , the simplest growth process of carbon clusters, could be observed from the time-resolved emission spectra of  $C_2$  (the Swan Band) generated by the laser vaporization of graphite.<sup>10</sup> In this paper we present detailed experimental evidence for the formation of  $C_2$  from  $2C_1$ . We have observed the  $2C_1 \rightarrow C_2$  process by means of both time-resolved emission spectra from the resulting  $C_2$  and the characterization of the products arising from the interaction of  $C_1$  and  $C_2$  with benzene. The mechanism for  $C_2$  formation will also be relevant to astrophysical applications, since  $C_2$  appears in carbon stars and interstellar clouds.<sup>11</sup>

### Experimental

#### Time-resolved Emission Spectra

The graphite surface was irradiated by the second harmonic from a YAG laser (532 nm, 10 Hz, 10 ns fwhm, LUMONICS) through a 30 cm focal length lens with varying laser powers (2.5, 3.4 and 5.0 mJ pulse<sup>-1</sup>), and the time-resolved spectra of the resulting emission were measured by a photodiode array detector with a gated system (Princeton Instruments: IRY 700G). The gate-width for detection of the photodiode array detector was set at 100 ns, and the time-resolved measurement was carried out by changing the delay time between the laser irradiation and the gate opening. The graphite sample was placed in a transparent cell, and continuously rotated to expose a fresh surface to the laser. The spectra were measured under argon and under a mixture of argon–benzene vapour generated by blowing argon into benzene at 27 °C.

#### Reaction Product Analysis

In a transparent glass vessel, shown schematically in Fig. 1, a graphite plate (7 × 30 × 3 mm<sup>3</sup>) was placed 3 mm above the

liquid benzene (condition A) or immersed in benzene (condition B). Argon was blown continuously into the liquid benzene. The second harmonic from a YAG laser (532 nm, 22 mJ pulse<sup>-1</sup>) was focused on the graphite surface through a lens of focal length 30 cm for 30 min. After laser irradiation, benzene was removed by evaporation.

The resulting concentrated solution was analysed by gas chromatography–mass spectrometry (GC–MS). A Varian 3400, with fused silica column (30 m × 0.255 mm, stationary liquid phase: SE-54), and a Finnigan MAT TSQ-70 were used as GC and MS, respectively. The column temperature was programmed to be set at 80 °C for 5 min, increased at 5 °C min<sup>-1</sup> for 14 min and then kept at 150 °C for 21 min.

The mass spectra were recorded by using electron ionization (ionization energy 70 eV) and chemical ionization (reagent gas: isobutane).

#### Emission and Time-of-flight Mass Spectra under Vacuum

To observe the emission spectra and time-of-flight (TOF) mass spectra immediately after the laser vaporization under vacuum ( $1.0 \times 10^{-7}$  Torr†), the graphite sample was placed between the acceleration electrode of the TOF mass spectrometer (R. M. Jordan) without any integration and cooling. On irradiation of the graphite with the 532 nm laser, both the emission spectra and TOF mass spectra were determined

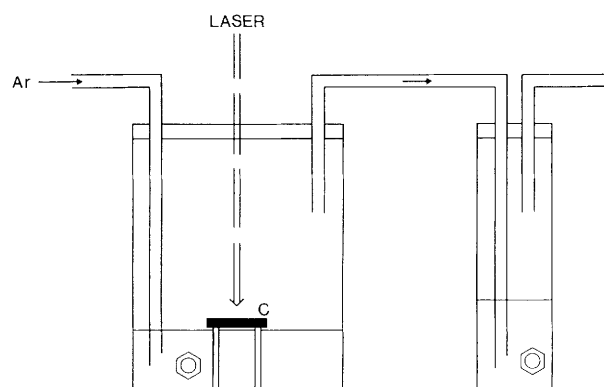


Fig. 1 Reaction vessel for reaction of benzene with species produced by laser vaporization of graphite

† 1 Torr = (101 325/760) Pa.

under the same conditions. The emission spectra were recorded by a photodiode array detector with a 1  $\mu\text{s}$  gate-width. The TOF mass spectra were measured without using a UV laser for ionization.

### Materials

Graphite (TOYO TANSO, ultra high purity graphite) and benzene (Wako, S) were used as received.

## Results and Discussion

### Observation of $\text{C}_2(\text{d}^3\Pi_g)$ Formation by Time-resolved Emission Spectra

#### Laser Vaporization of Graphite under Argon Atmosphere

Fig. 2(a)–(c) illustrate the time-resolved emission spectra from the graphite surface irradiated with laser powers of 2.5, 3.4 and 5.0  $\text{mJ pulse}^{-1}$ , respectively, under an argon atmosphere. The strong emission bands around 470 and 515 nm are in good agreement with the  $\Delta v = 1$  and  $\Delta v = 0$  sequences of the  $\text{C}_2(\text{d}^3\Pi_g \rightarrow \text{a}^3\Pi_u)$  Swan bands, respectively.<sup>12,13</sup>

The decay profiles of the Swan band observed on irradiation with different laser powers can be analysed according to first-order kinetics except for the first point at 0.5  $\mu\text{s}$ , and the resulting decay times, namely the reciprocal decay rate constants, are listed in Table 1. The decay time was increased from 2.3 to 4.3  $\mu\text{s}$  when the laser power increased from 2.5 to 5.0  $\text{mJ pulse}^{-1}$ . These decay times are much longer than the intrinsic lifetime of  $\text{C}_2(\text{d}^3\Pi_g)$ , nearly 110 ns as determined by the selective excitation of  $\text{C}_2(\text{a}^3\Pi_u \rightarrow \text{d}^3\Pi_g)$ ,<sup>14–16</sup> which indicates that the observed decay times are affected by the numbers of  $\text{C}_2(\text{d}^3\Pi_g)$  produced even at a few microseconds after the laser irradiation.

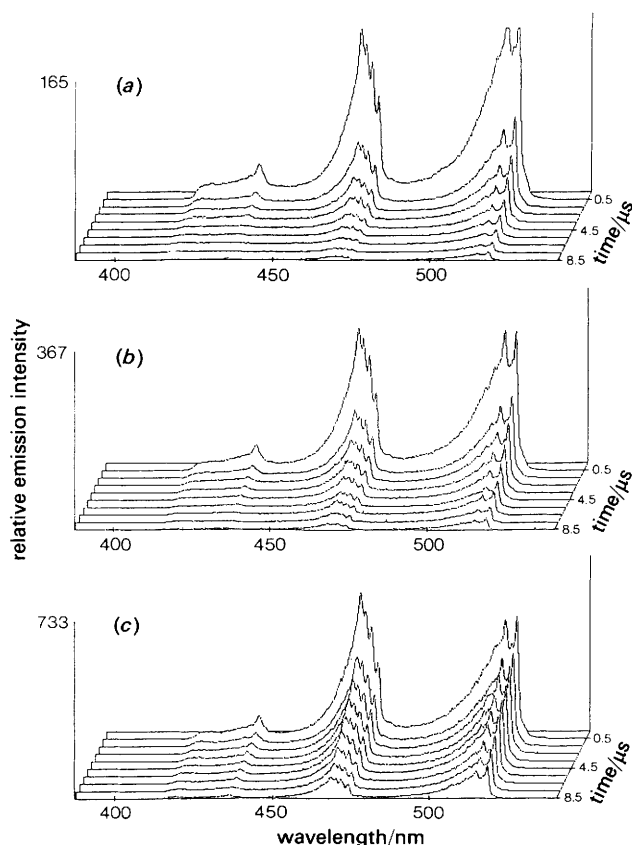
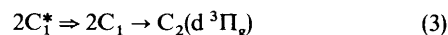
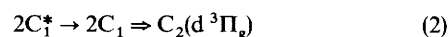


Fig. 2 Time-resolved spectra of the emission from the graphite surface irradiated with the second harmonic from a YAG laser under an argon atmosphere at room temperature. Laser power: (a) 2.5, (b) 3.4 and (c) 5.0  $\text{mJ pulse}^{-1}$ .

Table 1 Decay time (the reciprocal apparent first-order decay rate constant) of the  $\text{C}_2(\text{d}^3\Pi_g \rightarrow \text{a}^3\Pi_u)$  Swan band observed on irradiation of graphite with the second harmonic from a YAG laser under argon and argon–benzene atmospheres

laser power/ $\text{mJ pulse}^{-1}$	decay time/ $\mu\text{s}$	
	argon	argon–benzene
2.5	2.3	0.27
3.4	3.3	0.42
5.0	4.3	1.09

If  $\text{C}_2(\text{d}^3\Pi_g)$  or a much higher excited-state  $\text{C}_2$  was formed directly by the laser vaporization of the graphite, the observed decay time would be much shorter and decrease with increase in the laser power owing to the annihilation of the excited-state  $\text{C}_2$  molecules. Accordingly, it is clear that  $\text{C}_2$  results from the dimerization of  $\text{C}_1$  produced by the laser vaporization of graphite. There are three possible mechanisms for  $\text{C}_2(\text{d}^3\Pi_g)$  formation through the dimerization of  $\text{C}_1$  dependent on the rate-determining step.



( $\text{C}_1^*$ , higher excited-state of  $\text{C}_1$ ;  $\Rightarrow$ , rate-determining step)

If the dimerization process is the rate-determining step [eqn. (1) and (2)], the decay profile of the emission intensity will be analysed by second-order kinetics. However, the decay profile shown in Fig. 2 follows first-order kinetics; accordingly, mechanism (3) is the most probable, that is, the decay time observed in Fig. 2 to be much longer than the intrinsic lifetime of  $\text{C}_2(\text{d}^3\Pi_g)$  is due to the relaxation of highly excited  $\text{C}_1$ . The lifetime of excited-state  $\text{C}_1$ , longer than microseconds, is reasonable because the transitions  $^1\text{S} \rightarrow ^1\text{D}$  and  $^1\text{D} \rightarrow ^3\text{P}$  are forbidden,<sup>17,18</sup> and  $\text{C}_2(\text{d}^3\Pi_g)$  formation from  $2\text{C}_1(^3\text{P})$  is energetically allowed.<sup>19</sup> Accordingly, the decay profile observed in Fig. 2 corresponds to the concentration change of  $\text{C}_1$  at low-energy states.

#### Laser Vaporization of Graphite in the Presence of Benzene

In order to investigate the mechanism of  $\text{C}_2$  formation, the time-resolved emission spectra from the irradiated graphite surface were measured under an argon–benzene atmosphere, because benzene is known to react with  $\text{C}_1$ .<sup>20</sup> The spectra observed at laser powers of 2.5, 3.4 and 5  $\text{mJ pulse}^{-1}$  are shown in Fig. 3(a)–(c), respectively. The spectral shape is exactly the same as that under an argon atmosphere, shown in Fig. 2.

To demonstrate the effect of benzene on the decay time, the time profiles of the emission intensities at 470 nm determined under argon and under argon–benzene with a laser power of 3.4  $\text{mJ pulse}^{-1}$  are compared in Fig. 4. The decay profile under argon–benzene also gives a good fit to first-order kinetics. Table 1 lists the observed decay times in the presence of benzene at varying laser powers. As Fig. 4 and Table 1 show, the decay time is reduced in the presence of benzene. Furthermore, it was found that increase in the concentration of benzene vapour around the graphite reduced the decay time remarkably. This fact is attributed to the interaction of  $\text{C}_1$ , not  $\text{C}_2(\text{d}^3\Pi_g)$ , with benzene, because in the presence of benzene also the decay times observed are much longer than the intrinsic lifetime of  $\text{C}_2(\text{d}^3\Pi_g)$ . On reaction with benzene, the  $\text{C}_1$  concentration is quickly reduced, which subsequently decreases the number of  $\text{C}_2(\text{d}^3\Pi_g)$  produced from  $\text{C}_1$ .

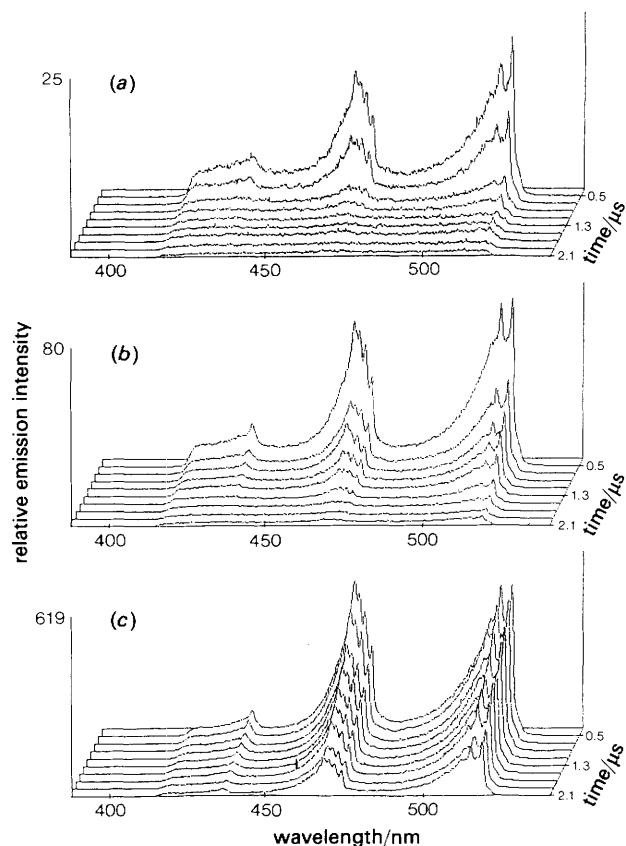


Fig. 3 Time-resolved spectra of the emission from the graphite surface irradiated with the second harmonic from a YAG laser under an argon–benzene atmosphere at room temperature. Laser power: (a) 2.5, (b) 3.4 and (c) 5.0 mJ pulse<sup>-1</sup>.

#### Reaction Products from Vaporized Graphite and Benzene

As described above, the time-resolved emission spectra under an argon–benzene atmosphere in Fig. 4 show that the vaporized carbon interacts with benzene. The product analysis using GC–MS provided clear evidence for the reaction between vaporized carbon and benzene; and the dependence of the reaction products on benzene concentration around the irradiated graphite gave an insight into the growth process,  $2C_1 \rightarrow C_2$ .

The laser was focused on the graphite placed either 3 mm above the liquid benzene surface (condition A) or immersed

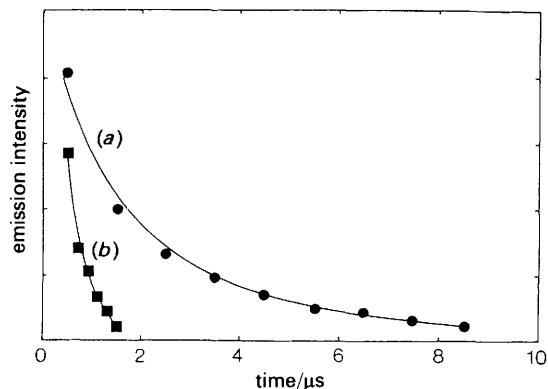
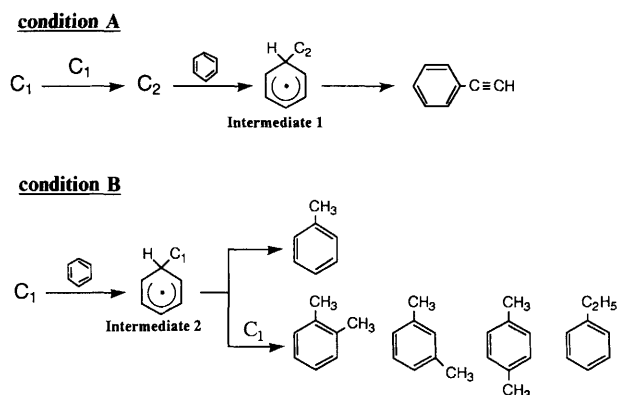


Fig. 4 Time profile of the emission intensity at 470 nm from the graphite surface irradiated with the second harmonic from a YAG laser (3.4 mJ pulse<sup>-1</sup>) under (a) an argon and (b) an argon–benzene atmosphere. The emission intensity of (b) is magnified by a factor of 3.3.

in the liquid benzene in the reaction vessel (condition B), as shown in Fig. 1. Table 2 lists the reaction products identified with their relative yields determined by the ion intensity of each peak in the mass chromatogram relative to that of phenylacetylene together with their retention times.

As Table 2 indicates, under condition A, phenylacetylene was the main product with xylenes and ethylbenzene as minor products. On the other hand, under condition B, the amounts of xylenes and ethylbenzene were comparable to that of phenylacetylene. The difference in the reaction mechanism between the conditions A and B is shown schematically below:



The concentration of benzene around the irradiated graphite under condition A is lower than that under condition B. Therefore, under condition A,  $C_1$  atoms vaporized from the graphite dimerize to give  $C_2$  before reacting with benzene, and the resulting  $C_2$  reacts with benzene to give phenylacetylene as the main product. Under condition B,  $C_1$  reacts efficiently with benzene to give considerable yields of xylenes and ethylbenzene in addition to toluene. Actually, the emission due to the  $C_2$  Swan band was observed during laser irradiation under condition A but was hardly observed under condition B.

The above difference in the product distribution between conditions A and B indicates that the growth process  $2C_1 \rightarrow C_2$  competes with the interaction of  $C_1$  with benzene. Styrene,  $C_6H_6-C_4$  ( $C_4$  or  $2C_2$  addition to benzene), biphenyl and diphenylacetylene will arise from the reactions of the intermediates 1 and 2 with benzene,  $C_2$  or the intermediates themselves, which occur more efficiently under condition B because of the cage effect of liquid benzene.

Table 2 Relative yields and retention times of the identified reaction products<sup>a</sup> on irradiation of graphite with the second harmonic from a YAG laser (532 nm, 22 mJ pulse<sup>-1</sup>) under conditions A and B (see text)

reaction products	retention time /min	relative yield	
		condition A	condition B
phenylacetylene	4.28	100	100
<i>o</i> -xylene	4.62	2	20
<i>m</i> - and <i>p</i> -xylene <sup>b</sup>	4.18	7	44
ethylbenzene	4.07	8	55
styrene	4.55	3	13
$C_6H_6-C_4$ <sup>c</sup>	12.50	20	90
biphenyl	18.83	14	115
diphenylacetylene	31.17	2	17

<sup>a</sup> Mass spectra and retention times except for  $C_6H_6-C_4$  were in good agreement with those of the authentic samples. <sup>b</sup> *m*- and *p*-xylene were not separated under the present conditions. <sup>c</sup>  $C_4$  or  $2C_2$  addition to benzene.

### Laser Vaporization of Graphite under Vacuum

The laser vaporization was carried out under vacuum ( $1.0 \times 10^{-7}$  Torr). Comparison of the results with those obtained under an argon atmosphere shows that the collisional relaxation of the excited-state  $C_1$  produced immediately after the laser irradiation plays an important role in the growth of  $C_1$  to  $C_2$ .

The second harmonic from a YAG laser ( $1.5 \text{ mJ pulse}^{-1}$ ) was directed through a lens of focal length 30 cm to the graphite surface which was placed at a graphite-lens distance  $l$  of 28.9 or 30.0 cm. The observed emission spectra, shown in Fig. 5, indicate that the laser power density affects the emission spectra remarkably. When the laser beam was not completely focused on the graphite surface ( $l = 28.9$  cm), the spectrum corresponds to the  $C_2$  Swan bands [Fig. 5(a)], which decay with a lifetime of  $\leq 200$  ns. On the other hand, when the laser beam was well focused on the graphite ( $l = 30.0$  cm), the spectrum is due to the transition of  $C_1^+(2s^24f \rightarrow 2s^23d)$  around 426 nm [Fig. 5(b)].<sup>21,22</sup>

TOF mass spectra were measured, under the same conditions as above, to determine the mass distribution of the carbon clusters resulting immediately after the laser irradiation. The resulting mass spectra are also strongly dependent on the laser power density at either  $l = 28.8$  or 30.0 cm, as illustrated in Fig. 6(a) and (b), respectively. At higher laser power density,  $C_1^+$  is predominantly observed. On the other hand, at lower laser power density, various carbon clusters,  $C_1^+$ ,  $C_3^+$ ,  $C_5^+$ ,  $C_7^+$  and  $C_{11}^+$ , are observed as prominent peaks as reported previously.<sup>23</sup>

Therefore, under vacuum, when the graphite is irradiated with higher laser power density,  $C_1$  is predominantly vaporized, and simultaneously ionized and excited to  $C_1^+(2s^24f)$  as observed in Fig. 5(b). The resulting  $C_1$  and  $C_1^+$  quickly disperse without growing carbon clusters. On the other hand, at lower laser power density,  $C_2$  is directly vaporized from the graphite, since the decay time of  $C_2(d^3\Pi_g \rightarrow a^3\Pi_u)$  emission,  $\leq 200$  ns, is close to the intrinsic lifetime of  $C_2(d^3\Pi_g)$ .

Under an argon atmosphere, the irradiation, even with much higher laser power density, does not give the emission of  $C_1^+(2s^24f \rightarrow 2s^23d)$ , but gives strong emission of  $C_2(d^3\Pi_g \rightarrow a^3\Pi_u)$  with much longer decay time than its

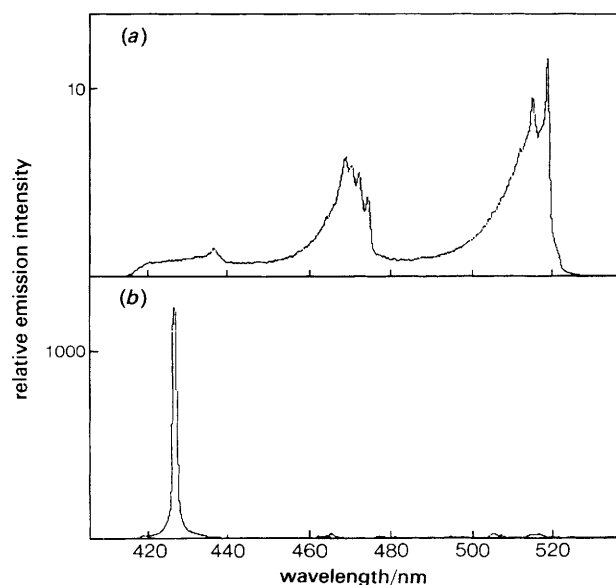


Fig. 5 Emission spectra from the graphite surface irradiated under vacuum ( $1.0 \times 10^{-7}$  Torr) with the second harmonic from a YAG laser ( $1.5 \text{ mJ pulse}^{-1}$ ) through a lens of focal length 30 cm. The graphite-lens distance ( $l$ ) was (a) 28.9 and (b) 30.0 cm.

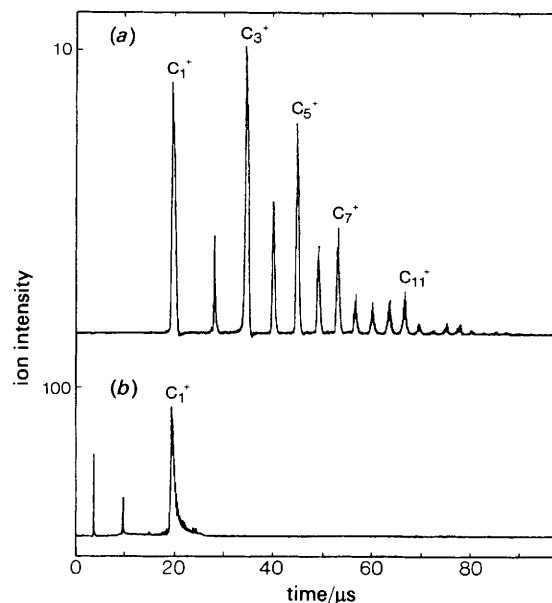


Fig. 6 TOF mass spectra of carbon clusters generated by the irradiation of graphite under vacuum ( $1.0 \times 10^{-7}$  Torr) with the second harmonic from a YAG laser ( $1.5 \text{ mJ pulse}^{-1}$ ) through a lens of focal length 30 cm. The graphite-lens distance ( $l$ ) was (a) 28.9 and (b) 30.0 cm.

intrinsic lifetime. This suggests that under an argon atmosphere, the resulting  $C_1$  deactivates to the ground state through collision with argon prior to its ionization, and then dimerizes to  $C_2$ .

### Conclusion

We have presented experimental evidence for the formation of  $C_2$  from  $2C_1$  as the simplest growth process of carbon clusters. Irradiation of a graphite plate with the second harmonic from a YAG laser under an argon atmosphere leads to strong emission of the  $C_2(d^3\Pi_g \rightarrow a^3\Pi_u)$  Swan band with much longer decay time than the intrinsic lifetime of  $C_2(d^3\Pi_g)$ .  $C_2$  is produced by dimerization of  $C_1$ ; the laser vaporization gives the higher excited state  $C_1$ , which is subsequently cooled to the ground-state  $C_1$  by collision with argon and then dimerizes.

Laser vaporization of graphite in the presence of benzene gives products arising from the action of  $C_1$  or  $C_2$  to benzene depending on the reaction conditions. The ratio of phenylacetylene to ethylbenzene and xylenes is higher at lower benzene concentration owing to the dimerization of  $C_1$  to  $C_2$  competing effectively with its reaction with benzene.

In contrast, under vacuum, the growth process,  $2C_1 \rightarrow C_2$ , does not occur, because the resulting higher excited state  $C_1$  is converted to excited  $C_1^+$ .

### References

- H. W. Kroto, J. R. Heath, S. C. O'Brien, R. F. Curl and R. E. Smalley, *Nature (London)*, 1985, **318**, 162.
- W. Krätschmer, L. D. Lamb, K. Fostiropoulos and D. R. Huffman, *Nature (London)*, 1990, **347**, 354.
- M. E. Geusic, M. F. Jarrold, T. J. McIlrath, R. R. Freeman and W. L. Brown, *J. Chem. Phys.*, 1987, **86**, 3862.
- K. Raghavachari and J. S. Binkley, *J. Chem. Phys.*, 1987, **87**, 2191.
- S. W. McElvany, B. I. Dunlap and A. O'Keefe, *J. Chem. Phys.*, 1987, **86**, 715.
- M. Doverstål, B. Lindgren, U. Sassenberg and H. Yu, *Z. Phys. D, Atoms, Molecules and Clusters*, 1991, **19**, 447.
- S. W. McElvany, *J. Chem. Phys.*, 1988, **89**, 2063.
- J. A. Zimmerman and W. R. Creasy, *J. Chem. Phys.*, 1992, **96**, 1942.

- 9 T. Wakabayashi and Y. Achiba, *Chem. Phys. Lett.*, 1992, **190**, 465.
- 10 A. Wakisaka, H. Sato, J. J. Gaumet, Y. Shimizu, Y. Tamori, M. Tsuchiya and K. Tokumaru, *J. Chem. Soc. Chem. Commun.*, 1993, 77.
- 11 E. F. VanDishoeck, *Ned. Tijdschr. Natuurkd. A*, 1985, **51**, 38.
- 12 W. Weltner Jr., P. N. Walsh and C. L. Angell, *J. Chem. Phys.*, 1964, **40**, 1299.
- 13 R. Bleekrode and W. C. Nieuwpoort, *J. Chem. Phys.*, 1965, **43**, 3680.
- 14 T. Tatarczyk, E. H. Fink and K. H. Beker, *Chem. Phys. Lett.*, 1976, **40**, 126.
- 15 W. Bauer, K. H. Beker, M. Bielefeld and R. Meuser, *Chem. Phys. Lett.*, 1986, **123**, 33.
- 16 C. Naulin, M. Costes and G. Dorthe, *Chem. Phys. Lett.*, 1988, **143**, 496.
- 17 P. S. Skell and R. R. Engel, *J. Am. Chem. Soc.*, 1965, **87**, 1135.
- 18 H. Yilmaz, *Phys. Rev.*, 1955, **100**, 1148.
- 19 J. M. Hollas, *Modern Spectroscopy*, Wiley, New York, 1992, p. 224.
- 20 J. L. Sprung, S. Winstein and W. F. Libby, *J. Am. Chem. Soc.*, 1965, **87**, 1812.
- 21 S. Bashkin and J. O. Stoner Jr., *Atomic Energy Levels and Grotorian Diagrams*, Elsevier, New York, 1975, p. 74.
- 22 H. Kayser, in *International Critical Tables of Numerical Data-Physics, Chemistry and Technology*, ed. E. W. Washburn, McGraw-Hill, New York, 1992, vol. 5, p. 285.
- 23 E. A. Rohlfing, D. M. Cox and A. Kaldor, *J. Chem. Phys.*, 1984, **81**, 3322.

Paper 2/06233J; Received 23rd November, 1992